

# Lawrence Berkeley National Laboratory

## Lawrence Berkeley National Laboratory

**Title**

RF Driven Multicusp H- Ion Source

**Permalink**

<https://escholarship.org/uc/item/8t1490vb>

**Author**

Leung, K.N.

**Publication Date**

1990-06-01



# Lawrence Berkeley Laboratory

UNIVERSITY OF CALIFORNIA

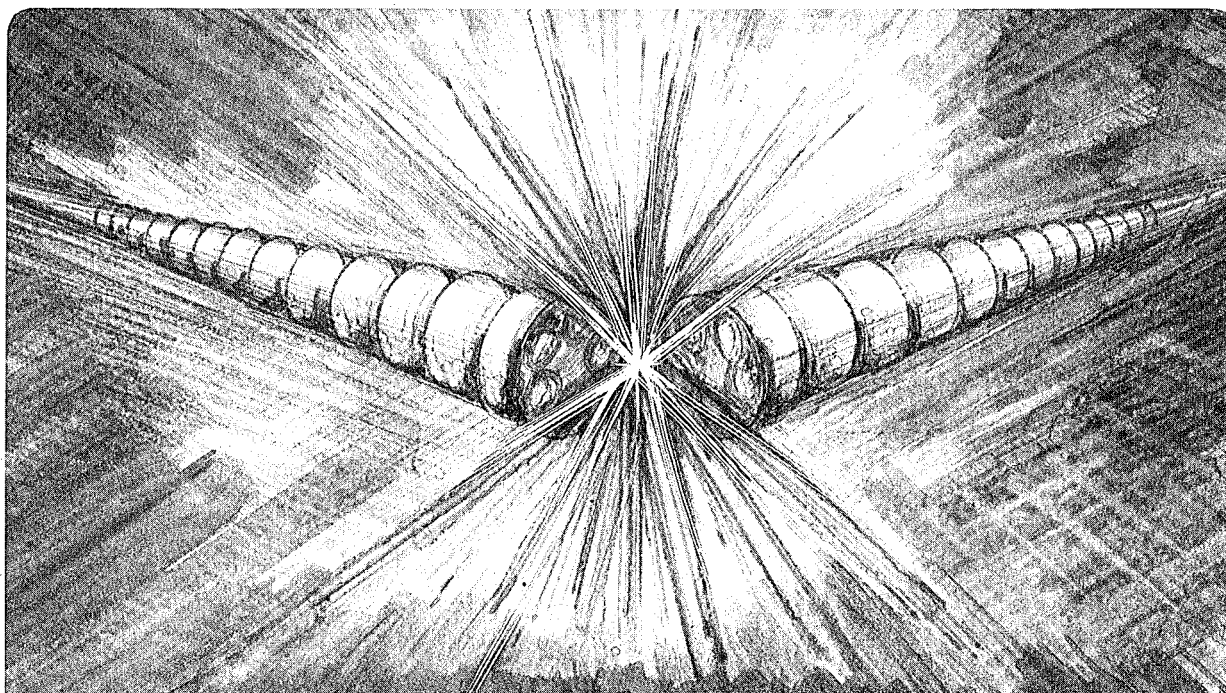
## Accelerator & Fusion Research Division

Submitted to Review of Scientific Instruments

### RF Driven Multicusp $H^-$ Ion Source

K.N. Leung, G.J. DeVries, W.F. DiVergilio, R.W. Hamm,  
C.A. Hauck, W.B. Kunkel, D.S. McDonald, and M.D. William

June 1990



#### **DISCLAIMER**

This document was prepared as an account of work sponsored by the United States Government. Neither the United States Government nor any agency thereof, nor The Regents of the University of California, nor any of their employees, makes any warranty, express or implied, or assumes any legal liability or responsibility for the accuracy, completeness, or usefulness of any information, apparatus, product, or process disclosed, or represents that its use would not infringe privately owned rights. Reference herein to any specific commercial products process, or service by its trade name, trademark, manufacturer, or otherwise, does not necessarily constitute or imply its endorsement, recommendation, or favoring by the United States Government or any agency thereof, or The Regents of the University of California. The views and opinions of authors expressed herein do not necessarily state or reflect those of the United States Government or any agency thereof or The Regents of the University of California and shall not be used for advertising or product endorsement purposes.

Lawrence Berkeley Laboratory is an equal opportunity employer.

RF Driven Multicusp H<sup>-</sup> Ion Source \*

K.N. Leung, G.J. DeVries, W.F. Divergilio, R.W. Hamm<sup>†</sup>, C.A. Hauck  
W.B. Kunkel, D.S. McDonald, and M.D. Williams

Lawrence Berkeley Laboratory  
University of California, Berkeley, CA 94720

<sup>†</sup> AccSys Technology Incl., Pleasanton, CA.

\* Work is supported by AccSys Technology, Inc., the Superconducting Super Collider Laboratory, and the Director, Office of Energy Research, Office of Fusion Energy, Development and Technology of Division, of the U.S. Department of Energy under Contract No. DE-AC03-76SF00098.



RF Driven Multicusp H<sup>-</sup> Ion Source

K. N. Leung, G. J. DeVries, W. F. DiVergilio, R. W. Hamm, C. A. Hauck,  
W. B. Kunkel, D. S. McDonald, and M. D. Williams

Lawrence Berkeley Laboratory  
University of California  
Berkeley, CA 94720

Abstract

An rf driven multicusp source capable of generating 1 msec H<sup>-</sup> beam pulses with a repetition rate as high as 150 Hz has been developed. This source can be operated with a filament or other types of starter. There is almost no lifetime limitation and a clean plasma can be maintained for a long period of operation. It is demonstrated that rf power as high as 25 kW could be coupled inductively to the plasma via a glass-coated copper-coil antenna. The extracted H<sup>-</sup> current density achieved is about 200 mA/cm<sup>2</sup>.

## Introduction

H<sup>-</sup> ion beams are required in fusion research and in several high energy accelerator projects. Multicusp plasma generators have been operated successfully both as volume production or surface conversion H<sup>-</sup> sources.<sup>1</sup> The H<sup>-</sup> ions generated by volume-production processes have lower beam emittance and thus are useful for the generation of high brightness beams. In order to achieve high current densities, volume H<sup>-</sup> sources require high discharge power.<sup>2</sup> For this reason, the lifetime of the filament cathodes is normally short for steady-state or high repetition rate pulse operations.

Radio-frequency (rf) antenna driven plasmas have been studied and developed at Lawrence Berkeley Laboratory (LBL) for the production of positive hydrogen ion beams.<sup>3</sup> An rf plasma source can be operated with a filament or other types of starter. There is almost no lifetime limitation and a clean plasma can be maintained for a long period of operation. The use of an rf plasma discharge as an H<sup>-</sup> source therefore is attractive for long time, pulsed or cw operations.

A new rf driven H<sup>-</sup> source has recently been developed at LBL for use in a calibration beam system and possibly in the injector unit of the Superconducting Super Collider (SSC). In order to meet the beam brightness and long and reliable operation requirement, we replaced the tungsten filaments with an antenna and generated the plasma by a 2 MHz induction discharge. The start-up time of the rf discharge is short and can be easily automated. To date, we have demonstrated that rf power higher than 25 kW could be coupled to the plasma via a glass-coated copper antenna. The highest extracted H<sup>-</sup> current density achieved was about 200 mA/cm<sup>2</sup>. This article describes the development and characteristics of this rf driven H<sup>-</sup> source.

## I. Experimental Setup

### A. The Ion Source Design

A schematic diagram of the ion source is shown in Fig. 1. The source chamber is a thin-walled copper cylinder (10 cm diam by 10 cm long) surrounded by 20 columns of samarium-cobalt magnets which form a longitudinal linecusp configuration for plasma confinement. The magnets, in turn, are enclosed by an outer anodized aluminum cylinder, with the cooling water circulating around the source between the magnets and the inner housing. The back flange has four rows of magnets cooled by drilled water passages. The source is designed for cw operation with a power input of 36 kW.

Magnetic field distribution inside the source chamber was analyzed by a computer code.<sup>4</sup> It was found that the discharge volume with magnetic field less than 30 G is approximately 6.5 cm in diameter. In order to achieve a quiescent discharge, the cathode for dc discharge operation is normally placed inside this central "field-free" region. In this study, the cathode was replaced by a three turn copper-coil antenna. Since the diameter of the coil was 6.5 cm, the rf antenna was located approximately within the boundary of the low-field region of the source.

In order to enhance the  $H^-$  yield, a pair of water-cooled permanent magnet filter rods was installed about 5 cm apart<sup>5</sup> (see Fig. 1). The filter rods provided a narrow region of transverse magnetic field which divided the entire source chamber into a discharge and extraction region. The filter field was strong enough to prevent energetic electrons from entering the extraction chamber. Excitation and ionization of the gas molecules took



place in the discharge chamber. Both positive and negative ions, together with cold electrons were present in the extraction region, and they formed a plasma with lower electron temperature, which is favorable for H<sup>-</sup> formation and survival.<sup>6</sup>

The open end of the source chamber was enclosed by a two-electrode extraction system. H<sup>-</sup> beams were extracted from the source through a 2-mm-diam aperture. A permanent-magnet mass analyzer was used with a Faraday cup (Fig. 1) to measure the electron and H<sup>-</sup> ion currents in the accelerated beam. The maximum extraction voltage used in this experiment was ~ 20 kV. In order to reduce the electron contents in the beam, a stainless-steel cylindrical collar (11.6 mm-diam by 9-mm-long) was installed at the exit aperture.<sup>7</sup> This collar has been optimized for filament discharge operation and it is capable of reducing the electron current by a factor of two without any degradation in the H<sup>-</sup> output current.

#### B. The RF Antenna

The rf antenna is typically fabricated from copper tubing and is then covered with a layer of insulating material. In this study, a three turn induction coil, fabricated from 4.7-mm-diam copper tubing was installed on the end flange (Fig. 2). The coil was adequately cooled by water for high power operation. There are two reasons for applying an insulating layer on the antenna. First, the insulation floats electrically at a much less negative potential than the antenna.<sup>8</sup> Thus, the degree of sputtering of the antenna material by plasma ions is considerably reduced. It was also observed that when the same antenna was operated without any insulation but under

similar source conditions, the ion density and therefore the efficiency of the source was reduced by a factor of two.<sup>8</sup> The reason for the drop in source efficiency when the bare antenna was used is still under investigation.

Since the peak voltage applied to the antenna can be very high, an ideal antenna coating should be able to withstand a high potential gradient between the plasma and the antenna. In the past, we have studied several coatings, namely; anodized aluminum, spun glass sleeving, ceramic coating, plasma sprayed ceramic coating and glass enamel coating.<sup>8</sup> The glass enamel coating proved to be by far the best insulating material against high-voltage breakdown. The thin uniform glass coating has a degree of flexibility which makes the coating resistant to cracking due to vibration. Moreover, the coefficient of thermal expansion of the glass enamel is sufficiently close to that of copper to afford a high degree of resistance to thermal stresses. Thus, the antenna is capable of withstanding a remarkably high thermal flux.

To form the thin glass enamel coating, the copper coil was first degreased, then acid cleaned to remove any oxide layer on the metal surface. A tacky organic binder was sprayed on the coil surface. This was followed immediately by the application of fine powdered glass frit on the entire antenna. The coil was then either resistively heated by an electric current or it could be heated externally inside an oven. When the coil temperature reached about 850 °C, the glass frit started to melt and eventually would "wet" the whole antenna surface. At this stage, the coil was removed from heating and allowed to cool. The melted frit now formed a thin solid glass coating on the copper coil with uniform thickness.

### C. The RF Power Supply System

The arrangement of the complete rf system is shown schematically in Fig. 3. A sine-wave oscillator drives a gated 400 W solid state amplifier at a nominal operating frequency of 1.8 MHz. The resulting rf pulses, with pulse width of up to 1 millisecond and repetition rate up to 150 pulses per second, drive a Class C tube amplifier with a maximum pulse output power of 30 kW.

The rf power is coupled to the antenna and matching circuit through a 30 kV isolation transformer. If the impedance of the source plasma is not properly matched to the rf generator, a large fraction of the rf power will be reflected back to the amplifier. In order to couple the rf power efficiently into the source plasma, a matching network (which is a tunable resonant parallel LC circuit) was employed.

The matching circuit is tuned to parallel resonance with the antenna representing about one third of the total inductance. The resistive part of the plasma load is matched to the 50  $\Omega$  source impedance by adjusting the excitation points on the external matching circuit coils. The reactive part of the plasma load shifts the resonant frequency of the matching circuit, and this effect is compensated by shifting the driving frequency. At this point, the difference in phase angle between the antenna voltage and current is a minimum.

If the source chamber pressure is high (>40 mTorr), a plasma can be easily produced by the rf pulses. However, if the hydrogen pressure is reduced to 15 mT or less, some auxiliary methods have to be employed for starting up the rf discharge. One might use a spark gap or perhaps a small high voltage induction coil for this purpose. In this experiment, we simply

installed a small 0.5-mm-diam hairpin tungsten filament on the back flange as illustrated in Fig. 2. A steady-state, very low density background plasma was generated by electron emission with a discharge voltage of ~60 V and discharge current of ~6 mA. All the data presented in the following sections were obtained with the source pressure optimized between 10 and 15 mTorr.

## II. Experimental Results

### A. Source Operation with Different Filter Magnets

The multicusp source is equipped with a pair of samarium-cobalt magnet filter rods which are placed 5 cm apart. This filter geometry was originally optimized for pure hydrogen dc discharges with a tungsten filament cathode.<sup>9</sup> When the source was operated with an rf discharge and with the same filter arrangement, Figure 4 shows the extracted H<sup>-</sup> current density first increased linearly with the rf input power. But the H<sup>-</sup> yield soon saturated when the power exceeded 15 kW. On the other hand, the extracted electron to H<sup>-</sup> ratio was approximately 60 for low rf power operations (Fig. 5). The ratio then increased rapidly for power higher than 15 kW and eventually reached 105 at 28 kW of rf input power.

The above observation indicates that the samarium-cobalt filter is not an optimized geometry for high power rf discharge operations. The filter field is too weak to maintain a low electron temperature plasma at the filter and extraction regions. In addition, the plasma potential could also become so positive that positive ions, together with electrons were leaking

through easily while  $H^-$  ions found it more difficult to reach the extraction region.

In order to increase the strength of the filter field, the samarium-cobalt magnets were replaced by similar size neodymium-iron magnets. As a result, the maximum B-field at the center of the filter was increased from 103 G to 130 G. According to the data shown in Fig. 4, the  $H^-$  current density was about the same as the samarium-cobalt filter for rf power below 6 kW. However, as the rf input power was increased from 6 to 28 kW, the  $H^-$  output for the neodymium-iron filter increased faster than that of the samarium-cobalt filter. Consequently, an extracted  $H^-$  current density as high as  $190 \text{ mA/cm}^2$  was obtained with 25 kW of rf power.

The data in Fig. 5 shows that there was also a significant reduction in the extracted electron to  $H^-$  ratio when the neodymium-iron magnet filter was used. For the range of rf power considered, the  $e/H^-$  ratio was always under 60. If higher rf power ( $>30 \text{ kW}$ ) is employed, the results shown in Figs. 4 and 5 suggested that an even stronger filter should be used so as to maintain a high  $H^-$  output and a low  $e/H^-$  ratio.

#### B. Comparison of Single and Multi-small-aperture Extraction System

The scaling of  $H^-$  current as a function of extraction area is of great interest in  $H^-$  source development. In a smaller (7.5-cm-diam) multicusp source, it has been found that as the extraction aperture size increases, the noise level of the accelerated  $H^-$  beam becomes very large.<sup>7</sup> Experimental investigation shows that the use of a multi-small-aperture arrangement at the extraction hole can greatly improve the quiescence of the the  $H^-$  beam.

In addition, when a 7-aperture extractor is compared with a single aperture, the  $H^-$  output is reduced only by 14% rather than 30% as expected due to the loss in transparency.<sup>7</sup>

In the new rf driven multicusp source, we have compared the extracted  $H^-$  current for source operation with a single and a 7-aperture arrangement. Figure 6 is a plot of the  $H^-$  current density as a function of rf input power. It can be seen that the  $H^-$  output is lower for the 7-aperture arrangement. Unlike the case of filament discharge, the reduction in  $H^-$  yield (~29%) is almost equal to the change in the overall transparency. Thus, for small extraction holes, there is no real advantage of using the multi-aperture configuration for rf driven plasmas.

### C. Comparison of RF and DC Filament Discharge Plasmas

The physics of  $H^-$  production in an rf discharge plasma is not well understood. There are no mono-energetic primary electrons present and the electron energy spectrum and the source plasma potential distribution are quite different from those of dc discharge plasmas. As a result, one would expect that the  $H^-$  ion yield and the  $e/H^-$  ratio could change significantly.

A dc discharge plasma was generated in the same source chamber by replacing the the rf antenna coil with a 1.5-mm-diam tungsten filament. The source was operated at a background pressure of 15 mTorr, with the discharge voltage maintained at 150 V and the discharge current varied between 50 and 150 A. Figure 7 shows some typical oscilloscope traces of the  $H^-$  and electron current for a 500- $\mu$ s pulse discharge operation. It can be seen that the shape of the  $H^-$  current is not uniform. It first

reached a maximum and then decreased to a lower value at the end of the pulse. A uniform  $H^-$  current pulse could be obtained if the source pressure was increased from 15 to 20 mTorr. The time-dependent behavior of the  $H^-$  current is not yet understood and it is still under investigation.

Figure 8 is an oscilloscope picture showing the  $H^-$  and electron current during a 500- $\mu$ s rf discharge pulse. Unlike dc filament discharge, the shape of the  $H^-$  pulse was very uniform even though the source pressure was maintained at 15 mTorr. When the rf plasma was operated at a pressure either higher or lower than 15 mTorr, the  $H^-$  current level would decrease but the pulse shape always remained uniform.

The maximum  $H^-$  output current for both rf induction and dc filament discharges is summarized in Fig. 9. When compared with the same input power, rf discharges generally produced higher  $H^-$  currents (>40%) than dc filament discharges. The extracted electron to  $H^-$  ratios are about the same for the range of discharge power tested (Fig. 10).

Previously, it has been found that for positive hydrogen ion beam production, the  $H^+$  ion fraction and power efficiency are about the same for rf and dc discharge plasmas when operated with the same source geometry.<sup>3</sup> Hence, the plasma density in an rf induction discharge should be about the same or perhaps lower than that of a dc filament discharge (depending on the electron temperature). A higher  $H^-$  output would indicate that an rf induction discharge could generate more vibrationally-excited  $H_2$  molecules in the main source chamber which in turn result in more  $H^-$  formation. Additional measurements on the electron energy, plasma potential and vibrationally-excited molecule distributions are planned to give us a better understanding of the characteristics of this rf driven  $H^-$  source.

In conclusion, we have demonstrated that an rf driven multicusp source can generate volume-produced H<sup>-</sup> ions with extracted current densities as high as 200 mA/cm<sup>2</sup>. Higher H<sup>-</sup> output should be achievable if a higher power rf amplifier is available. This type of ion source is reliable, easy to operate and has a long lifetime. If the H<sup>-</sup> beam emittance is proven to be the same as that of dc discharge operations, then this rf induction driven source should be extremely useful for the production of high brightness H<sup>-</sup> beams.

### **Acknowledgment**

We would like to thank D. Moussa, S. Wilde, P. Rosado and P. Purgalis for technical assistance. This work is supported by AccSys Technology Inc., the Superconducting Super Collider Laboratory and the Director, Office of Energy Research, Office of Fusion Energy, Development and Technology Division, of the U.S. Department of Energy under Contract No. DE-AC03-76SF00098.

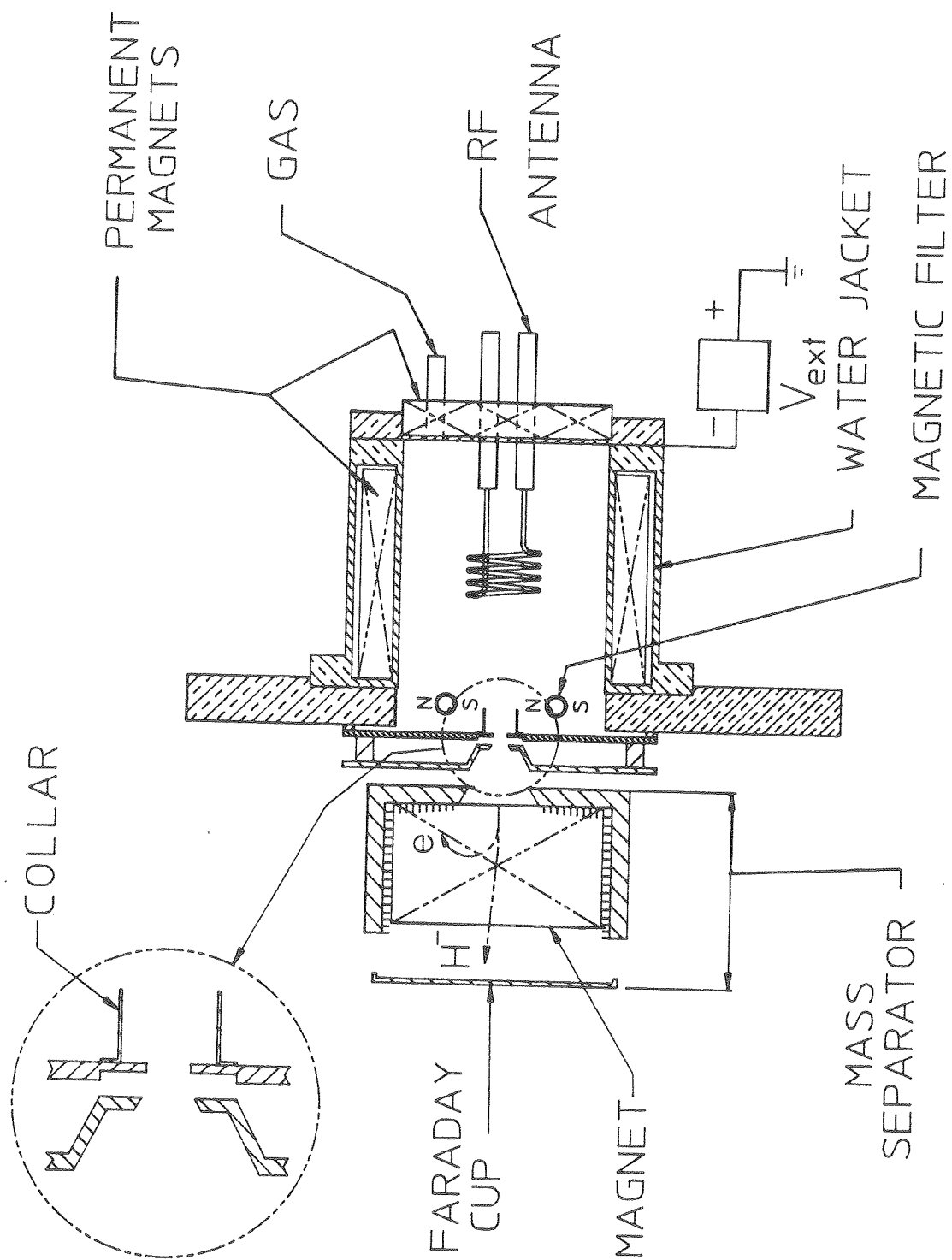


## Reference

1. K. N. Leung, Nucl. Instrum. and Meth. B40/41, 1028 (1989).
2. K. N. Leung, K. W. Ehlers, C. A. Hauck, W. B. Kunkel, and A. F. Lietzke, Rev. Sci. Instrum. 59, 453 (1988).
3. M. C. Vella, K. W. Ehlers, D. Kippenhan, P. A. Pincosy, R. V. Pyle, W. F. DiVergilio and V. V. Fosnight, J. Vac. Sci. Technol. A3(3), 1218 (1985).
4. K. N. Leung, O. A. Anderson, C. F. Chan, W. S. Cooper, G. J. DeVries, C. A. Hauck, W. B. Kunkel, J. W. Kwan, A. F. Lietzke, P. Purgalis, and R. P. Wells, Rev. Sci. Instrum. (Sept. 1990).
5. K. N. Leung, K. W. Ehlers, and M. Bacal, Rev. Sci. Instrum. 54, 56 (1983).
6. J. R. Hiskes and A. M. Karo, J. Appl. Phys. 56, 1927 (1984).
7. K. N. Leung, C. A. Hauck, W. B. Kunkel, and S. R. Walther, Rev. Sci. Instrum. 61, 1110 (1990).
8. K. N. Leung, K. W. Ehlers, D. Kippenhan, and M. C. Vella, J. Vac. Sci. Technol. A2(2), 675 (1984).
9. K. N. Leung, C. A. Hauck, W. B. Kunkel, and S. R. Walther, Rev. Sci. Instrum. 60, 531 (1989).

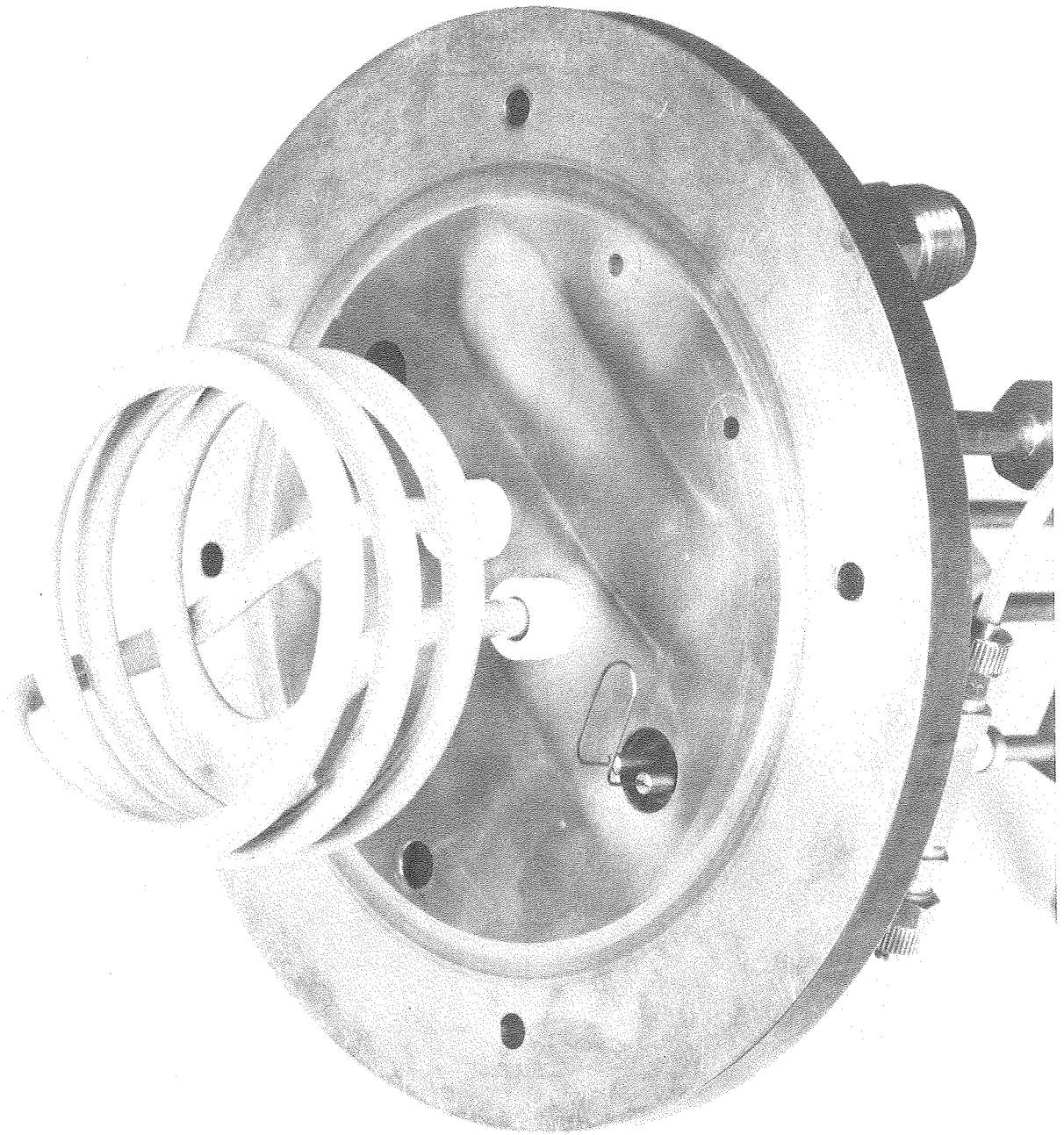
## Figure Captions

- Fig. 1 Schematic diagram of the multicusp ion source modified for operation with an rf induction coil.
- Fig. 2 A picture showing the glass-coated induction coil installed on the back flange of the ion source. The small tungsten filament is used for starting the rf discharge.
- Fig. 3 Schematic diagram of the complete rf power system.
- Fig. 4  $H^-$  output as a function of rf power for two different filter magnets.
- Fig. 5 Ratio of extracted electrons to  $H^-$  ions as a function of rf power for two different filter magnets.
- Fig. 6  $H^-$  output as a function of rf power for a single and a seven aperture extraction arrangement.
- Fig. 7 Oscilloscope traces showing the extracted electron and  $H^-$  current, the discharge voltage and current for a 500- $\mu$ s pulse dc filament discharge.
- Fig. 8 Oscilloscope traces showing the extracted electron and  $H^-$  current for a 500- $\mu$ s rf pulse discharge.
- Fig. 9 Comparison of  $H^-$  output for rf and filament discharge operations.
- Fig. 10 Comparison of the extracted electron to  $H^-$  ratio for rf induction and dc filament discharge operations.



XBL 907-2418

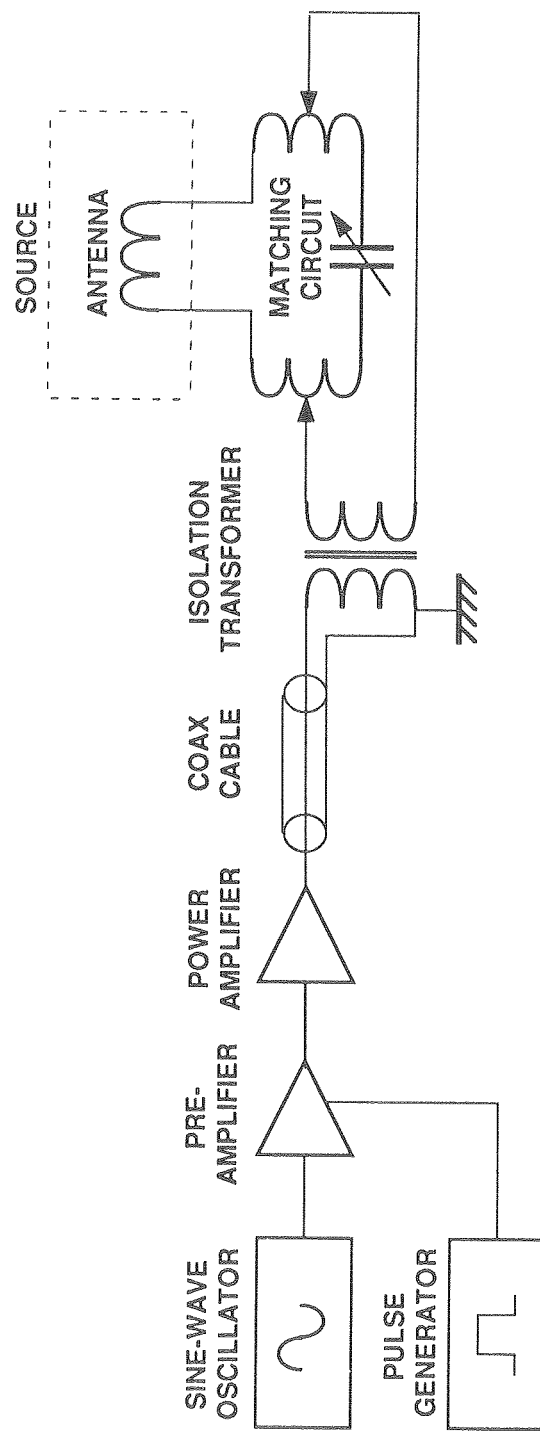
Fig. 1 Schematic diagram of the multicusp ion source modified for operation with an rf induction coil.



1 2 3 4 5 6 7 8 9  
CENTIMETERS LBL

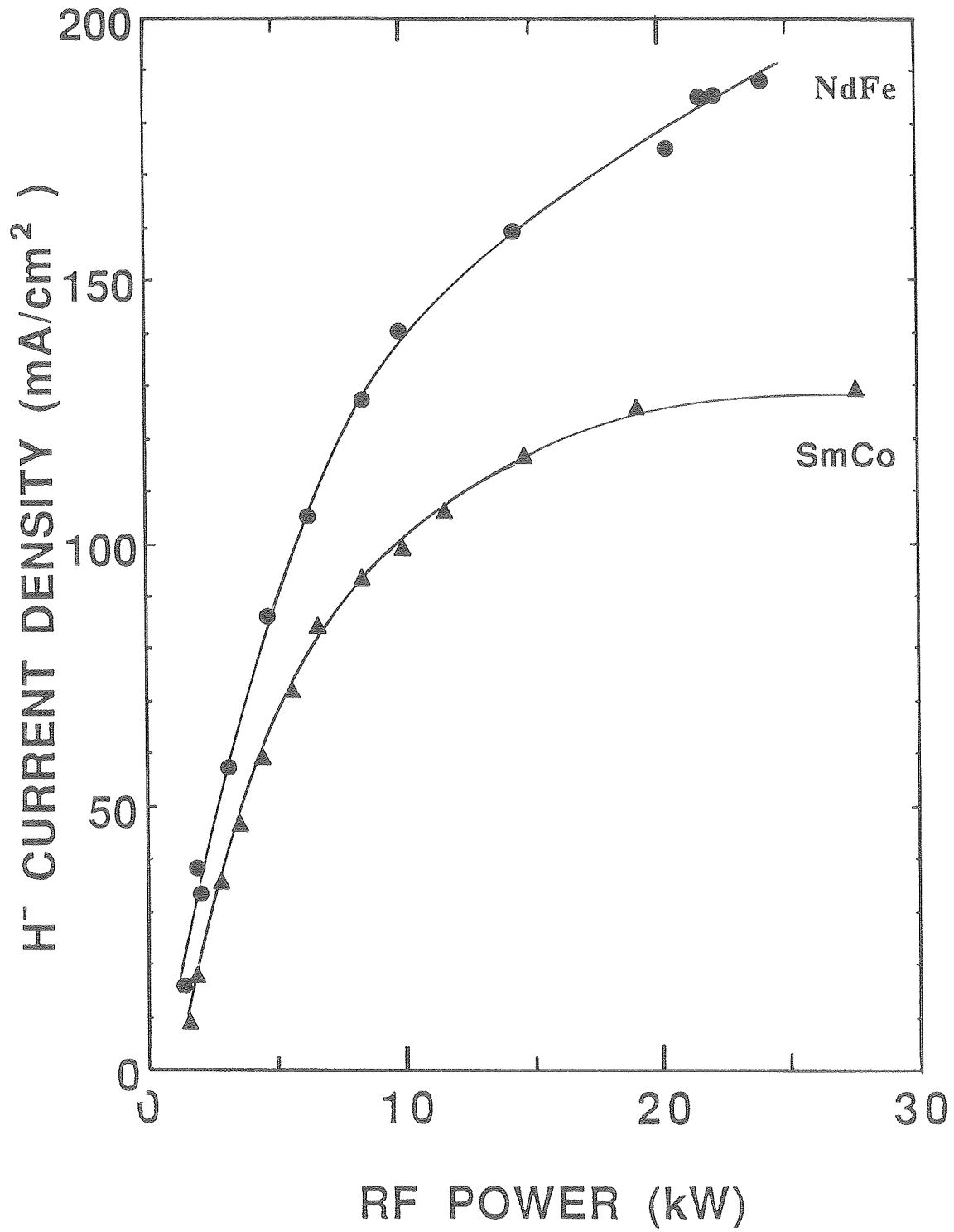
CBB 901-389

Fig. 2 A picture showing the glass-coated induction coil installed on the back flange of the ion source. The small tungsten filament is used for starting the rf discharge.



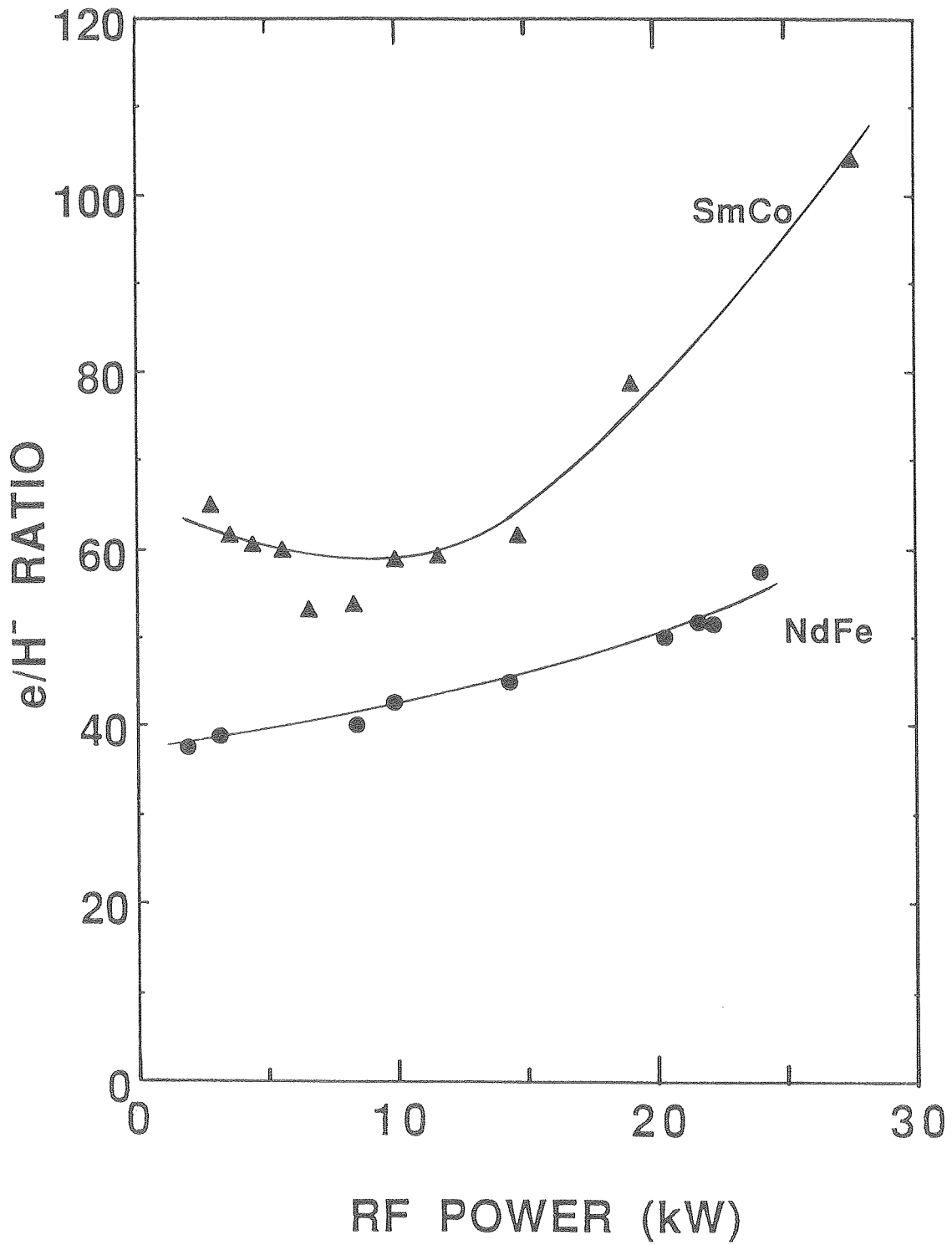
XBL 907-2408

Fig. 3 Schematic diagram of the complete rf power system.



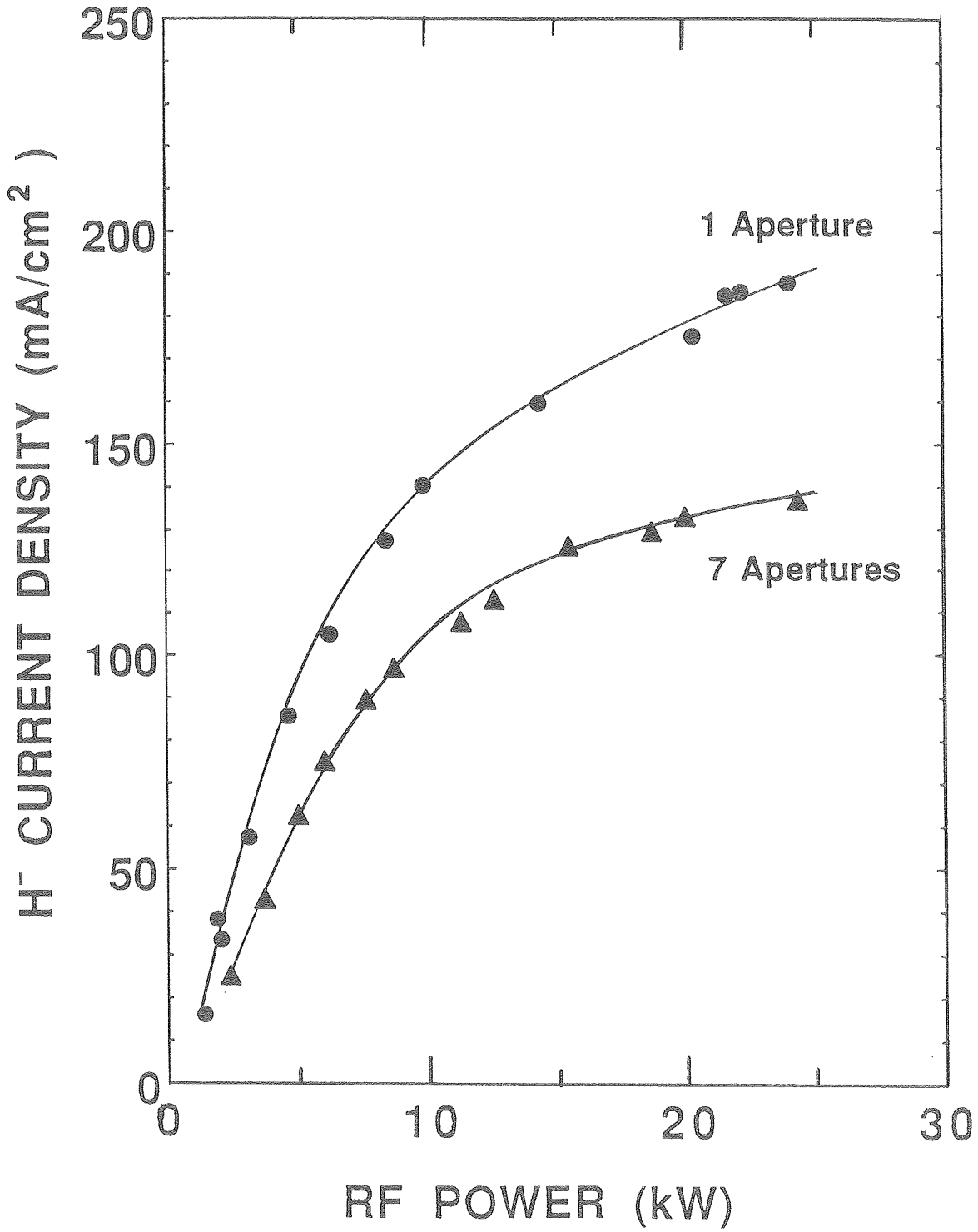
XBL 907-2414

Fig. 4 H<sup>-</sup> output as a function of rf power for two different filter magnets.



XBL 907-2416

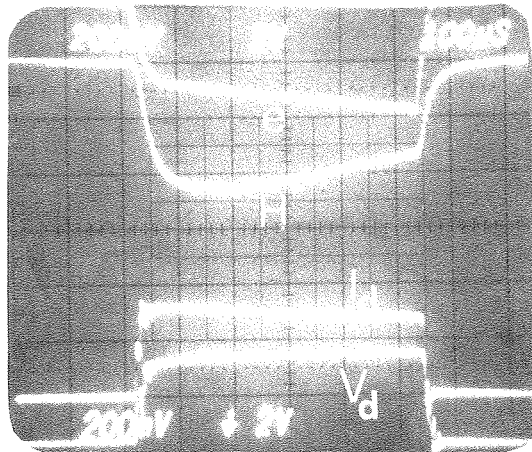
Fig. 5 Ratio of extracted electrons to H<sup>-</sup> ions as a function of rf power for two different filter magnets.



XBL 907-2415

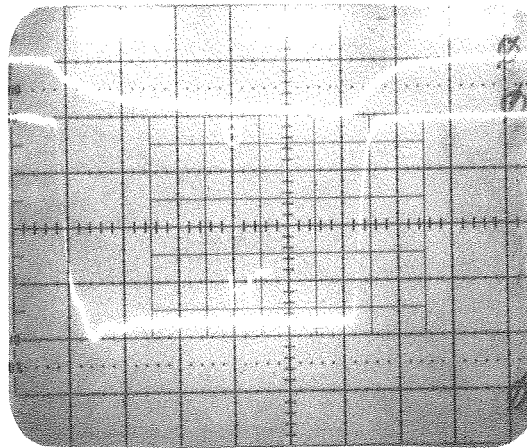
Fig. 6 H<sup>-</sup> output as a function of rf power for a single and a seven aperture extraction arrangement.





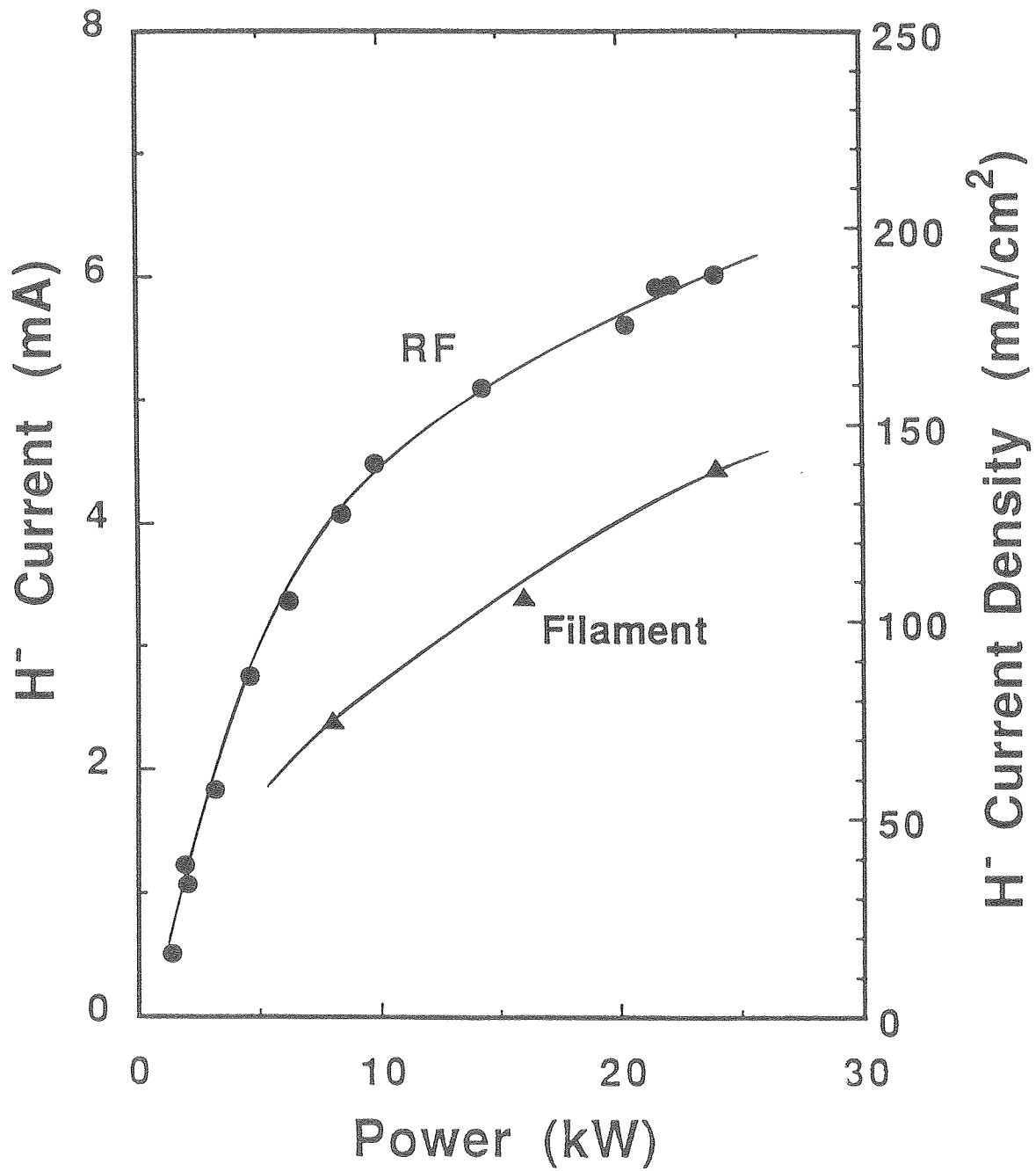
XBB 907-5583

Fig. 7 Oscilloscope traces showing the extracted electron and  $H^-$  current, the discharge voltage and current for a 500- $\mu s$  pulse dc filament discharge.



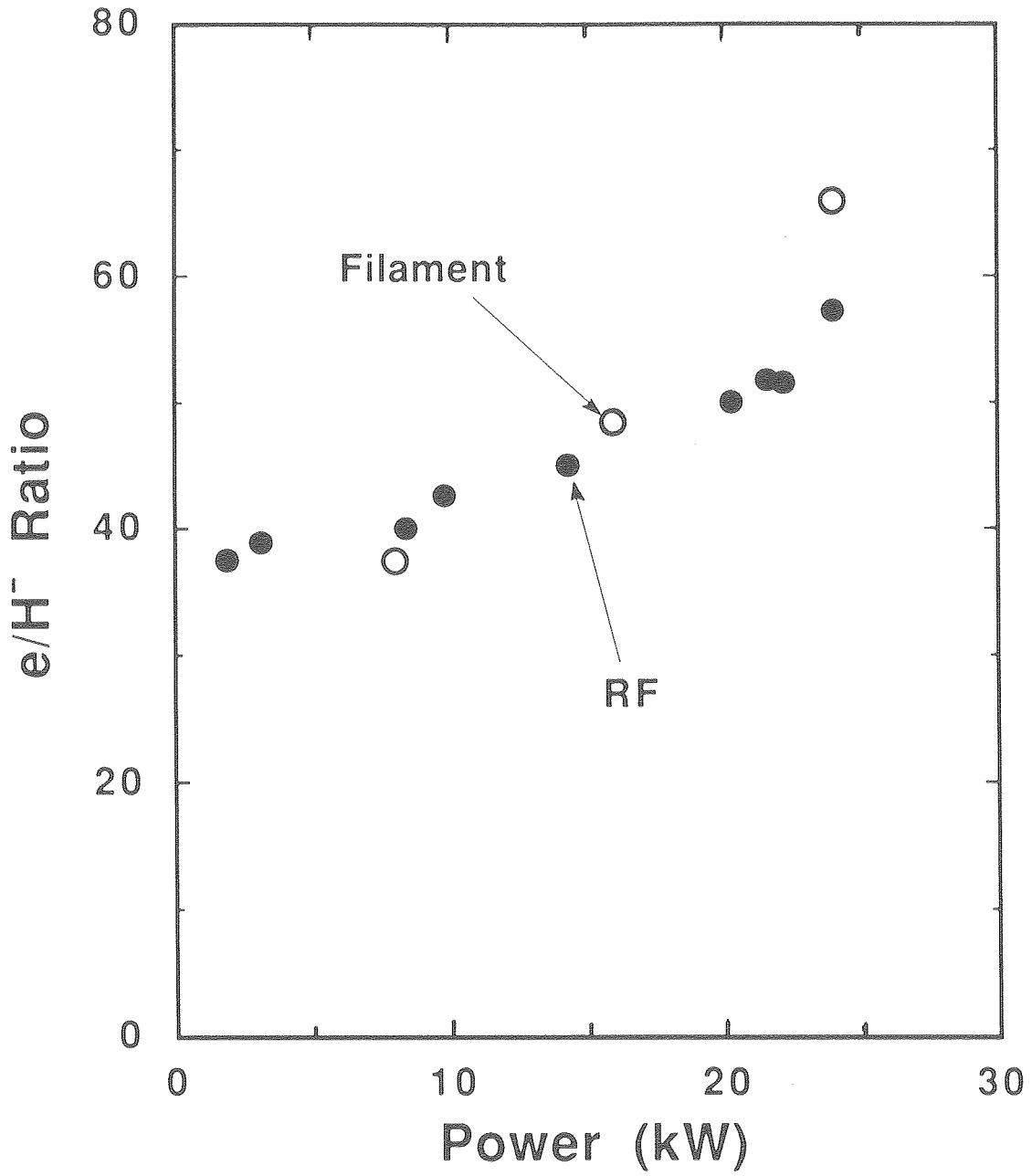
XBB 907-5584

Fig. 8 Oscilloscope traces showing the extracted electron and  $H^-$  current for a 500- $\mu s$  rf pulse discharge.



XBL 907-2417

Fig. 9 Comparison of H<sup>-</sup> output for rf and filament discharge operations.



XBL 907-2409

Fig. 10 Comparison of the extracted electron to H<sup>-</sup> ratio for rf induction and dc filament discharge operations.

This report was done with support from the United States Energy Research and Development Administration. Any conclusions or opinions expressed in this report represent solely those of the author(s) and not necessarily those of The Regents of the University of California, the Lawrence Berkeley Laboratory or the United States Energy Research and Development Administration.